

Sequential Monte Carlo sampling for crack growth prediction providing for several uncertainties

Matteo Corbetta¹, Claudio Sbarufatti², Andrea Manes³, and Marco Giglio⁴

^{1,2,3,4}*Politecnico di Milano, Dipartimento di Meccanica, Milan, 20156, Italy*

*matteo.corbetta@polimi.it
claudio.sbarufatti@polimi.it
andrea.manes@polimi.it
marco.giglio@polimi.it*

ABSTRACT

The problem of fatigue crack growth monitoring and residual lifetime prediction is faced by means of sequential Monte Carlo methods commonly defined as sequential importance sampling/resampling or particle filtering techniques. The algorithm purpose is the estimation of the fatigue crack evolution in metallic structures, considering uncertainties coming from phenomenological aspects and material properties affecting the process. These multiple uncertainties become a series of unknown parameters within the framework of the dynamic state-space model describing the crack propagation. These parameters, if correctly estimated within the particle filtering algorithm, will cover the uncertainties coming from the real environment, improving the prognostic performances. The standard particle filter formulation needs additional methods to augment the state vector and to correctly estimate the parameters. The prognostic system composed by the sequential Monte Carlo algorithm able to account for different uncertainties is tested through several crack growth simulations. The applicability of the method to real structures and the employment in presence of real environmental conditions (i.e. variable loading conditions) is also discussed at the end of the paper.

1. INTRODUCTION

Crack propagation is one of the most widespread phenomena affecting metallic structures. Engineering community dedicated a lot of effort into the comprehension of the fracture mechanism and crack propagation phenomena, especially when fatigue loads affect the cracked structure. The latter case is well known as the fatigue crack growth (FCG) or fatigue crack propagation problem and, intuitively, it causes the need of the time to failure and the residual useful

life (RUL) of the cracked structure for maintenance and safety purposes.

The most part of RUL estimation techniques based on fracture mechanics have been developed from the work of Paris & Erdogan (1963) describing the crack growth rate as a function of the stress intensity factor (SIF) range acting during a fatigue load cycle. In the last decades, many works have been dedicated to FCG dealing with multiple aspects. Nonetheless, in spite of these in-depth studies, the RUL predictions cannot overlook the statistical aspects of fatigue crack propagation. The variability affecting FCG was highlighted from Virkler, Hillberry, Goel (1978), when 68 fatigue crack growth tests on Al2024-T3 specimens produced a large variability of the crack growth data. This scatter can increase exponentially dealing with real structures in real environments. As a matter of fact, there are different sources of uncertainty affecting the fatigue crack behavior: (i) the variability of the material properties, (ii) the load sequences, (iii) the environmental conditions and (iv) the intrinsic variability of the phenomenon, that is driven by nano-scale events not accounted for within the usual engineering models.

In order to overcome this variability and to improve the time to failure and RUL predictions, several statistical methods have been developed. Statistical definition of FCG parameters is a very popular technique to address the crack growth variability, since the parameter values comes from fitting procedures like regressions, maximum likelihood estimations etc. (Cross, Makeev & Armanios 2007, Corbetta, Sbarufatti, Manes & Giglio, 2014). Other methods employ stochastic models of the crack, using both analytical solutions and Monte Carlo methods, (Ray & Patankar 1999, Scafetta, Ray & West 2006, Mattrand & Bourinet, 2011).

As mentioned above, the difficulties increase dealing with variable loading conditions. Elber (1970, 1971) introduced the crack closure effect that it has been studied later in presence of variable amplitude loading conditions by Newman (1981). Fatigue crack propagation under variable or

Matteo Corbetta et al. This is an open-access article distributed under the terms of the Creative Commons Attribution 3.0 United States License, which permits unrestricted use, distribution, and reproduction in any medium, provided the original author and source are credited.

random loading conditions is still an open issue nowadays. Apart from the Newman's paper (1981), many other works dedicated to crack growth rate are available (Newman 2005, Willenborg, Engle & Wood, 1971) and more recent papers appeared highlighting new methods to describe the prediction of crack propagation under random load spectra (Newman, Irving, Lin & Le, 2006, Mattrand & Bourinet, 2011). Nowadays, the development of real-time Structural Health Monitoring (SHM) techniques paves the way to real-time prognostics of structures. From a structural reliability point of view, the final target of prognostics is the prediction of the structure RUL starting from the information provided by an SHM unit composed by localized or distributed sensor networks and diagnostic algorithms. The output information should be combined with advanced algorithms able to take into account the uncertainties coming from both the SHM unit and the uncertainties affecting the monitored process. Therefore, the estimation of the probability density function (pdf) of the residual lifetime becomes feasible. The two main approaches employed in prognostics are the *data-driven* approach and the *model-based* approach. The first uses large amount of data to train algorithms able to predict the future degradation trends based on the previous knowledge, the second takes advantage of physical or phenomenological models to predict the most probable damage evolution. Only the *model-based* approach is considered in this context, based on the large number of studies on FCG and available models.

Considering the SHM-Prognostics framework, a Sequential Importance Resampling (SIR) algorithm is proposed in this paper to track the damage propagation and update the RUL estimation of a simple structure subjected to fatigue loads. The dynamic state-space (DSS) model of the system is proposed in an *adaptive* form, thanks to the adaptation of model parameters and random processes. These quantities will be estimated during the crack propagation thanks to dedicated techniques within the SIR algorithm. Similar algorithms have just been applied to the fatigue crack growth problem. Cadini, Zio & Avram (2009) have applied *particle filter* algorithm (in the form of Sequential Importance Sampling/Resampling – SIS/SIR) without the parameter estimation. Corbetta, Sbarufatti, Manes & Giglio proposed a SIS/SIR algorithm with stochastic DSS model (2013a) and updating of the model parameters through Markov chain Monte Carlo (MCMC) techniques (2013b). Chiachio, Chiachio, Saxena, Rus & Goebel (2013) proposed a more complicated prediction problem dealing with composite materials and combined state-parameter estimation within the DSS framework. The SIR algorithm proposed in this work have some novelties with respect to the cited works, making use of the concept of *intra-specimen* and *inter-specimen* variability introduced by Bourinet & Lemaire (2008) and explained in detail in section 2. The *artificial dynamics* (AD) just used by Daigle & Goebel (2011) and Chiachio et al. (2013), and the *kernel smoothing* (KS) techniques will

improve the knowledge of the DSS model parameters describing the crack evolution. These methods will try to cover the inter-specimen variability affecting different specimens of the same structure. The intra-specimen variability is covered by a *dynamic noise variance* within the SIR formulation, explained in detail in section 3.4. An additional novelty introduced by this work is the evaluation of the Residual Useful Life through the numerical solution of the stochastic integral proposed by Yang & Manning (1996) instead of the long-lasting step-by-step simulation of the crack growth. Unfortunately, this method works in presence of constant-amplitude fatigue loads only. The purpose of this algorithm is to try covering several sources of uncertainties that can appear on real structures subjected to crack propagation. Several virtual tests on crack propagation altered with respect to the theoretical crack growth curve will prove the validity of the method.

The paper organizes as follows: section 2 briefly introduces the FCG equation and its intrinsic variability, focusing on the residual life prediction problem. Section 3 summarizes sequential Monte Carlo methods and Bayesian filtering estimation, describing the adopted techniques for combined state-parameter estimations and dynamic noise variance selection. Section 4 shows the application of the algorithm to a simulated crack propagation and the prognostic formulation. Section 5 is dedicated to the results of the algorithm in terms of parameter estimation and RUL prediction, comparing the *artificial dynamics* and the *kernel smoothing* techniques. Section 6 concludes the paper.

2. PROBLEM STATEMENT: FATIGUE CRACK GROWTH MONITORING AND PREDICTION

Several FCG models are able to describe the growth rate as a function of crack length and a series of model parameters. The most popular model is the Paris-Erdogan equation (Paris & Erdogan, 1963) describing the FCG rate per load-cycle using the SIF range affecting the crack tip, as defined in Eq. (1a), and two empirical parameters commonly defined as C and m , as visible in Eq. (1b).

$$\Delta K(x) = F(x)\Delta S\sqrt{\pi x} \quad (1a)$$

$$\frac{dx}{dN} = C[\Delta K(x)]^m \quad (1b)$$

Where x is the current crack length, ΔS is the applied load range, $F(x)$ is a crack shape function depending on the crack length and the structure geometry, and N is the general load cycle. If the load range has constant amplitude and constant frequency, the FCG rate domain can easily change from load cycle to time domain, and Eq. (1b) becomes a first-order ordinary differential equation. If the discrete-time domain is used to describe the crack evolution, Eq. (1b) changes into Eq. (2a)¹, where the crack growth rate dx/dN follows the

¹ Supposing a relatively small number of cycles ($\Delta N \rightarrow 1$).

Paris-Erdogan Eq. (1b) or any other FCG rate model (see for instance the NASGRO model, NASA J.S. Centre, 2002).

Considering the RUL of the cracked component, the Paris-Erdogan model allows the direct calculation of the remaining number of cycles by a direct integration of Eq. (1b) using the separation of variable method, Eq. (2b)².

$$x_k = x_{k-1} + \frac{dx}{dN} \Big|_{x=x_{k-1}} \Delta N \quad (2a)$$

$$N_r = \frac{x_{lim}^{(1-\frac{m}{2})} - x_0^{(1-\frac{m}{2})}}{CF^m \Delta S^m \pi^{\frac{m}{2}} \left(1 - \frac{m}{2}\right)} \quad (2b)$$

The term x_0 indicates the starting crack length, x_{lim} is the limit crack length governed by the fracture toughness and the safety requirements for the structure. N_r is the number of remaining load cycles needed to reach the length x_{lim} starting from x_0 . All the other variables are the same as in Eqs. (1). The application of more complicated models makes unfeasible the direct integration of Eq. (1b), requiring numerical integration or Monte Carlo simulation to estimate the remaining cycles. Obviously, the deterministic definition of N_r cannot be employed in effective lifetime predictions or maintenance strategies, because of the large variability affecting the crack growth process. As a proof of the variability affecting the FCG process on real structures, Figure 1 shows some experimental results coming from fatigue crack growth tests on helicopter fuselage panels. The ordinate axes shows the crack length in millimeters as a function of the load cycles on the abscissa. As clearly visible, there is an high discrepancy between the theoretical curve (built with NASGRO model) and the experimental data. Therefore, a statistical approach is mandatory for an efficient residual lifetime prediction. The interested reader can refer to Corbetta et al. (2014) for further information about the mentioned experimental activity.

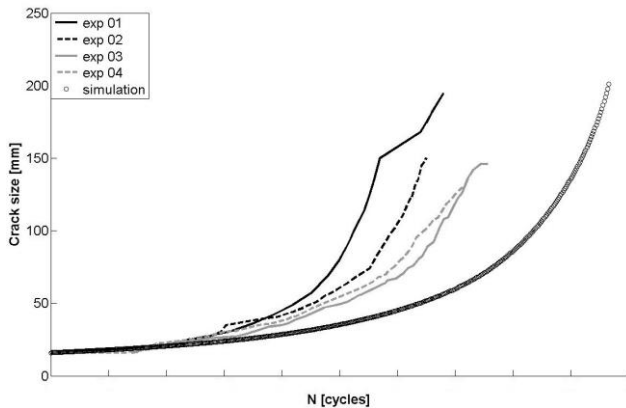


Figure 1. Comparison between experimental data and theoretical crack growth curve built with NASGRO model.

² Considering a constant shape function $F(x) = F$.

2.1. Conceptual definition of fatigue crack growth variability

According to the previous considerations on the scatter affecting FCG data, the Bourinet & Lemaire (2008) approach is proposed here with a little modification. The method can be applied with any kind of FCG propagation model that follows the general form $dx/dN = g(x)$ (in load-cycle domain or time domain).

The variability affecting crack propagation is split into two main contributions, each of them related to one or several sources of uncertainty, according to the Bourinet & Lemaire approach. Firstly, a crack evolution can differ from the theoretical one because of different values of material properties and/or empirical parameters, which cannot be described by a single value for all the structures built with the same material. It is easy to understand this concept giving thought to a large fleet of the same aircraft, or to all the metallic parts constituting a long bridge or an high-rise building. Even though the same material is used, uncertainties due to manufacturing processes and environmental uncertainties are always present in these kind of structures. Moreover, as just mentioned above, the crack propagation event follows a random behavior caused by several variability not considered in the common engineering models of the phenomenon. This random behavior produces discrepancies between the theoretical crack evolution and the expected one, and these discrepancies can appear in a small time-range. The two variability contributions are defined as *inter-specimen* variability and *intra-specimen* variability, respectively.

2.1.1. Inter-specimen variability

Usually, the *inter-specimen* variability is described within the FCG model by a randomization of the parameters, for instance C and m affecting the Paris-Erdogan model. This is the most common technique to produce a random FCG model, and the sequential information on the crack length updates the parameter pdfs by means of statistical tools. Corbetta et al. (2014) propose an Adaptive Markov chain Monte Carlo algorithm to update the parameter distributions during real crack propagation on portions of helicopter fuselage. On the other hand, a slightly different approach is proposed hereafter. Checking the discrete-form of crack evolution in Eq. (2a), it can be described as in Eq. (3).

$$x_k = x_{k-1} + \Delta x_{k-1} \Delta N \quad (3)$$

Where Δx_{k-1} is the result of the Paris-Erdogan model in this context. Actually, $\Delta x \cdot \Delta N$ describes the crack increment within few load cycles. The model used to evaluate the crack increment Δx can be very complex and composed by a large quantity of empirical parameters and/or material properties; however, the result will be always a crack increment per load

cycle (or per time unit considering constant-amplitude loads). Now, consider that the monitoring of the crack and the subsequent RUL prediction are the main goal of the prognostic system. Thus, one might be not interested in the exact knowledge of the parameters describing the current crack propagation, as the main intent is to correctly monitor the damage and to improve the prognostic performances. Accordingly, the inter-specimen variability is described hereby a single mathematical constant called *correction parameter* ψ . It will be modulated according to the information related to the crack length during the crack propagation. The correction parameter ψ multiplies the crack increment Δx to adjust the model prediction on the measures coming from a general diagnostic unit (Eq. (4a)). The proposed Paris-Erdogan formulation is highlighted in Eq. (4b).

$$x_k = x_{k-1} + \psi_{k-1} \Delta x_{k-1} \Delta N \quad (4a)$$

$$x_k = x_{k-1} + \psi_{k-1} C (F(x) \Delta S \sqrt{\pi x_{k-1}})^m \Delta N \quad (4b)$$

The updating procedure will change the value of the correction parameter ψ instead of the two parameters C and m during the Bayesian filter operation. The correction parameter, will try to cover the inter-specimen variability affecting the crack propagation phenomenon. From a different point of view, it could be considered a drift of the process noise usually employed to generate the stochastic model. This drift should cover the bias between the expected crack evolution (driven by the deterministic parameters of the model) and the actual crack growth happening on the structure.

2.1.2. Intra-specimen variability

The *intra-specimen* variability can be represented by a random process altering the crack growth at each time step as just presented by Yang & Manning (1996). The FCG rate model is modified by a lognormal random noise Ω , Eq. (5a).

The employment of a lognormal random process to describe Ω is due to the nature of the damage. In fact, cracks can only increase over time (or at least, they remain constant), thus the crack increment during a discrete time step cannot be negative. Others distributions are able to satisfy this requirement, however the lognormal distribution is the easiest way to introduce the correct variability affecting the crack growth process. This random noise is representative of all the possible uncertainties affecting the real environments with respect to the theoretical model describing the FCG phenomenon: variability of the actual state of stress near the crack, environmental conditions, different direction of the applied load with respect to the expected one, just to name a few of them.

Equation (3) modifies according to Ω and it can be employed in a dynamic state-space model of the process, Eq. (5b).

$$\frac{dx}{dN} = \Omega C [\Delta K(x)]^m \quad (5a)$$

$$x_k = x_{k-1} + C [\Delta K(x_{k-1})]^m \omega_{k-1} \Delta N \quad (5b)$$

Where the term ω_{k-1} in Eq. (5b) is a realization of the random process Ω . This variable represents the random noise of the process within the Bayesian filtering framework. Even in this case, the optimal value of the process noise is unknown at the beginning of the crack growth. The first moments of the random noise (for instance the mean and variance) should be properly tuned using previous experimental tests representative of the current condition of the system. However, the amount of uncertainty makes impossible a complete characterization of the random noise. Then, the mean and the variance associated to the random noise Ω will be estimated during the crack propagation according to the data coming from the observation equation, as described in section 3.

2.1.3. Residual useful life prediction

The integration of Paris-Erdogan model is feasible even if the model becomes a random process due to the presence of Ω . The lognormal random process introduced in Eq. (5a) is used to evaluate the probability density function of the RUL according to Eq. (2b). As introduced by Yang & Manning, the integration of $dx/dN = \Omega g(x)$ brings to the equivalence in Eq. (6).

$$\int_{x_0}^{x_{lim}} \frac{1}{g(x)} dx = \int_0^{N_r^0} \Omega dN \quad (6)$$

The term N_r^0 is the theoretical number of remaining load cycles calculated with the deterministic FCG rate model $g(x)$. The RUL distribution could be evaluated by means of Monte Carlo sampling and the theory of stochastic processes, avoiding the step-by-step simulation of crack growth samples commonly implemented in standard SIS/SIR algorithms. As a matter of fact, the right-hand side of Eq. (6) can be approximated using the summation of $n^* = N_r^0/\Delta N$ samples coming from the process Ω multiplied by the discretization ΔN , as in Eq. (7).

$$\int_0^{N_r^0} \Omega dN \approx \sum_{j=1}^{n^*} \omega_j \Delta N \quad (7)$$

Again, the term ω_j is the j -th sample coming from the random process Ω . The repetition of the summation in Eq. (7) for a relatively large number of times produces an approximation of the probability density function of the RUL in agreement with the theoretical curve defined by the stochastic Paris-Erdogan law in Eq. (5a). This simple approach is limited to the case of constant amplitude loading conditions, and it will be explained in detail in section 3 within the pseudo-code of the SIR algorithm (subsection 3.5). Thus, if variable loads are applied to the cracked components, the step-by-step

simulation of the crack should be adopted, as well as more complicated techniques to evaluate the stochastic integrals.

3. SEQUENTIAL IMPORTANCE RESAMPLING, PARAMETER ESTIMATION AND ADAPTIVE NOISE VARIANCE

Literature about sequential Monte Carlo sampling is vast at least as the literature on fatigue crack growth. Therefore, the section summarizes the main features of SIR algorithms with a focus on the crack monitoring and prediction problem only.

3.1. Monitoring and Prediction from a Bayesian filtering perspective

Equations (3-5) presented in section 2 can be generalized with the common dynamic state-space model formulation composed by the state evolution, Eq. (8a) (following the hypothesis of the hidden Markov models of order one) and the observation equation, that is Eq. (8b) (linking the actual state of the system with the information provided by a measurement system).

$$x_k = f(x_{k-1}, \theta, \omega_{k-1}) \quad (8a)$$

$$z_k = h(x_k, \eta_k) \quad (8b)$$

The vector θ contains empirical parameters supposed to be constant during the system evolution. Variables z_k represents the measure related to the state x_k at the general k -th step, and η_k is the random noise affecting the measurement system. The objective within the formulation of Bayesian filters is the evaluation of the posterior probability density function of the state x given a series of noisy observations z at a general time-step k ; it means the calculation of $p(x_k|z_{1:k})$. From a mathematical viewpoint, the problem statement is described by the Chapman-Kolmogorov equation, Eq. (9a) and the subsequent updating via Bayes' rule, Eq. (9b).

$$p(x_k|z_{1:k-1}) = \int p(x_k|x_{k-1})p(x_{k-1}|z_{1:k-1})dx_{k-1} \quad (9a)$$

$$p(x_k|z_{1:k}) = \frac{p(x_k|z_{1:k-1})p(z_k|x_k)}{p(z_k|z_{1:k-1})} \quad (9b)$$

The analytical solution of the posterior pdf is available if the system is linear and the processes are described by Gaussian distributions. This is not the case for crack propagation phenomena. The SIR algorithm allows approximating the posterior distribution $p(x_k|z_{1:k})$ by a series of samples representative of the system state, usually called *particles* by the widespread definition of the algorithm *particle filter*. Each particle has an associated weight w depending on the sequential information coming from the measurement system, diagnostic unit etc. The approximation of the posterior pdf is expressed in Eq. (10).

$$p(x_k|z_{1:k}) \approx \sum_{i=1}^{N_S} w_{n,k}^{(i)} \delta(x_k - x_k^{(i)}) \quad (10)$$

Where N_S is the total number of particles, $x_k^{(i)}$ is the value of the i -th particle at the general k -th time step, $w_{n,k}^{(i)}$ is the

normalized weight associated to that particle and δ is the Dirac delta-function. The weight formulation employed in the SIR algorithm agrees with the bootstrap approximation, in which the transition density from x_{k-1} to x_k is used as proposal distribution for the sample generation (Haug, 2005). As a consequence, the weights depend on the value at the previous step $k-1$ and on the likelihood of the measure given the particle value, as shown in Eq. (11).

$$w_k^{(i)} = w_{k-1}^{(i)} p(z_k|x_k^{(i)}) \quad (11)$$

Then the weights are normalized such that $\sum w_k^{(i)} = 1$. Arulampalam, Maskell, Gordon & Clapp (2002) and Doucet, Godsill & Andrieu (2000) produced a detailed description of the algorithm for the interested reader.

In case of combined state-parameter estimation, the vector x is augmented such that the *extended system state* is represented by the damage state and the parameter variables $y_k = [x_k, \theta]$. Particles associated to the state $x^{(i)}$ and the parameter sample $\theta^{(i)}$, together with the related weight $w^{(i)}$, will be representative of the combined state-parameter estimation or *extended system state*, Eq. (12a). It has to be remarked that the subscript k associated to θ in Eq. (12a) indicates the value of θ at the general k -th step, and it does not mean that θ is time-varying. The weight updating follows the same procedure of the standard particle filtering, nevertheless the likelihood of the measure is affected by the value of $\theta^{(i)}$ used to propagate the particle (Eq. (12b)).

$$\{y_k^{(i)} = (x_k^{(i)}, \theta_k^{(i)})\}_{i=1}^{N_S} \quad (12a)$$

$$w_k^{(i)} \propto w_{k-1}^{(i)} p(z_k|y_k^{(i)}) = w_{k-1}^{(i)} p(z_k|x_k^{(i)}, \theta_k^{(i)}) \quad (12b)$$

The combined state-parameter posterior pdf is expressed thanks to Bayes' rule (13) as highlighted by Liu & West (2001).

$$p(y_k|z_{1:k}) \propto p(z_k|y_k)p(x_k|\theta, z_{1:k-1})p(\theta|z_{1:k-1}) \quad (13)$$

As clearly visible by Eq. (13), the knowledge of the parameter pdf given the series of observations z is fundamental to approximate the posterior pdf of the augmented state vector y correctly. Thus, the proposal distribution from which to draw the samples of the parameter vector has to be considered in the SIR algorithm. The next sub-section briefly discusses the two main approaches used in this work: the *artificial dynamics* and the *kernel smoothing* techniques (Liu & West, 2001). Both these techniques will be used during the algorithm to update the *correction parameter* ψ shown in section 2. They have been selected because of their simplicity, while other more advanced techniques are available in literature as summarized by Kantas, Doucet, Singh & Maciejowski (2009).

3.2. Artificial dynamics technique

The main drawback in the insertion of constant parameter in the state vector is that the filtering method has to identify two

different quantities: one is time-varying, and the other one is constant. The first attempt is to select a DSS equation for the constant parameter on the form $\theta_k = \theta_{k-1}$. However, it leads to the well-known problem of *sampling impoverishment* or *sample degeneracy*. The *sample degeneracy* can be overcome by the addition of a small change in the sample values at each step of the algorithm. This small change is a random noise added to each particle, as presented in Eq. (14).

$$\theta_k^{(i)} = \theta_{k-1}^{(i)} + \xi_k^{(i)} \quad (14)$$

where $\xi_k^{(i)}$ is a random value with zero-mean and a variance that decreases in time. This is the idea suggested by Gordon, Salmond & Smith (1993) and recalled by Liu & West (2001). Actually, the statistics of ξ does not depend on the observed data, then $p(\theta|z_{1:k-1})$ is negligible in the posterior formulation of the state distribution.

Noticeably, the simplicity of the method introduces a non-negligible drawback that is the loss of information between the time steps. It happens because of the introduction of the mentioned artificial changing in the parameter values when they are fixed. Moreover, two questions have to be solved to maximize the performances of the algorithm: the selection of the initial covariance matrix of ξ , $\sigma_{\xi,0}^2$, and the decreasing function depending on the discrete time $\sigma_{\xi}^2 = \sigma_{\xi,0}^2 f(k)$, in order to reach the convergence in a relatively small number of iterations.

3.3. Kernel smoothing technique

Kernel smoothing method was developed by West (1993b) and it is based on the mixture modelling approach. It allows approximating the parameter posterior distribution by a Gaussian mixture using the weights associated to the particles, as shown in Eq. (15).

$$p(\theta|z_{1:k}) \approx \sum_{i=1}^{N_S} w_k^{(i)} N(\theta|\mu_{\theta,k}^{(i)}, \zeta_k^2 \Sigma_{\theta,k}) \quad (15)$$

where $\mu_{\theta,k}^{(i)}$ is the *kernel location* for the i -th particle of the parameter θ , ζ_k is the *smoothing parameter* and $\Sigma_{\theta,k}$ is the Monte Carlo covariance matrix of θ . Intuitively, $N(\cdot|\mathbf{m}, \mathbf{S})$ indicates a probability that follows a normal distribution with mean \mathbf{m} and covariance matrix \mathbf{S} . Effective kernel locations $\mu_{\theta,k}$ are specified according to the *shrinkage rule* proposed by West (1993b) depending on the smoothing parameters ζ_k and another parameter $\mathbf{b} = \sqrt{(1 - \zeta_k^2)}$. Equation (16) defines the kernel location for each particle.

$$\mu_{\theta,k}^{(i)} = \mathbf{b} \theta_{k-1}^{(i)} + (1 - \mathbf{b}) E(\theta_{k-1}) \quad (16)$$

The term $E(\theta_{k-1})$ is the mean of the parameter vector θ at the $k-1$ th time step. Even though this methodology allows an effective and adaptive sampling technique, the function $\zeta_k = \zeta(k)$ must be properly selected in order to reach the convergence of the algorithm. It should be a small decreasing function of the time as it happens for the variance introduced

in the *artificial dynamics* method. Nevertheless, the loss of information is limited with respect to the previous approach.

3.4. Dynamic noise variance

In the previous sub-section, the problem of constant parameter estimation is faced presenting two different techniques covering the *inter-specimen* variability affecting the damage propagation phenomenon that can appear on real structures. Now the focus is on the *intra-specimen* variability. In this kind of nonlinear problems with non-Gaussian pdfs, the selection of too small noise features makes the algorithm unable to track the state variations properly. If this happens, the wrong state estimation will produce larger errors in the estimation of the RUL. On the other hand, too large noise features produce unreasonable enlargement of the posterior distributions, then useless information. Moreover, a too large noise variance alters the particle evolutions producing implausible propagation of the crack and falling into unexpected RUL distribution, too. An adaptive noise is proposed hereafter, trying to avoid the tuning of the noise Ω affecting the process.

A suitable process noise for the crack growth problem is the lognormal random process already introduced in section 2. According to the theory of lognormal distributions, Ω can be described as an exponential function of a normal random process Λ , with mean and variance precisely selected, Eqs. (17a, b). In order to produce an unbiased estimation of the mean crack growth curve, the mean and variance of the normal random process Λ must be related according to the formulation in Eq. (17c), such that the mean of the random process approaches one (Eq. (17d)).

$$\Omega = \exp \Lambda \quad (17a)$$

$$\lambda \sim N(\mu_{\Lambda}, \sigma_{\Lambda}^2) \quad (17b)$$

$$\mu_{\Lambda} = -\frac{\sigma_{\Lambda}^2}{2} \quad (17c)$$

$$E(\Omega) = \exp\left\{\mu_{\Lambda} + \frac{\sigma_{\Lambda}^2}{2}\right\} = 1 \quad (17d)$$

In this way, the average of the random process x (the evolution equation of the DSS model) will be centered on the deterministic evolution of x . The i -th sample of the process noise ω can be easily drawn according to Eq. (18).

$$\omega^{(i)} \sim \exp\{\lambda^{(i)}\} = \exp\{\mu_{\Lambda} + \sigma_{\Lambda} r\} \quad (18)$$

Where r indicates a random value drawn from the standardized normal distribution; thus $\lambda^{(i)}$ is a single realization of the random process Λ . Despite the link between the mean and the variance of the random process, the selection of σ_{Λ}^2 remains heuristic in the common practice. Then, a non-constant variance tuned on the scatter of the measures could improve the performance of the algorithm.

According to this concept, the simulations presented in section 5 make use of two methods to adjust the noise variance. First, the variance of the process Λ is assumed equal to the variance associated to the observations, which is a function of the estimated state at the previous time-step, as expressed in Eq. (19).

$$\sigma_{\Lambda_{k+1}}^2 = \sigma_{z_k}^2(x_k) \quad (19)$$

This is a very simple approach useful for systems where the variance of the process or the variance of the measurement system can increase over time, like in the structural degradation processes. The other technique makes use of the formulation of Xu and Li (2005) introducing the *similarity parameter* between the observation and the estimated state, defined in Eq. (20). The similarity parameter is proportional to the distance between $E(x_k)$ and the observation z_k in multi-dimensional or one-dimensional spaces (as in this case). The term $V(x_k)$ indicates the Monte Carlo variance of the state at time step k .

$$\varphi_k = \exp\left\{-\frac{(z_k - E(x_k))^2}{2V(x_k)}\right\} \quad (20)$$

The new noise variance is computed according to Eq. (21) through the *similarity parameter* φ_k .

$$\sigma_{\Lambda_{k+1}}^2 = \max\left(\min\left(\sigma_{\Lambda_0}^2 \sqrt{\frac{1}{\varphi_k}}, \sigma_{\Lambda,max}^2\right), \sigma_{\Lambda,min}^2\right) \quad (21)$$

Actually, the variance selection is replaced by the tuning of three parameters, so it is not completely avoided. They are the constant $\sigma_{\Lambda_0}^2$, the maximum and minimum allowable variances, $\sigma_{\Lambda,max}^2$ and $\sigma_{\Lambda,min}^2$. However, the selection of these quantities could be simpler than the selection of the optimal variance in some cases. Both the formulations in Eq. (19) and Eq. (21) will be employed in the SIR algorithm.

3.5. Algorithm operation

Sub-sections 3.1-3.4 define the equations adopted in the SIR algorithm, highlighting the artificial dynamics and kernel smoothing techniques to estimate constant model parameters (covering the *inter-specimen* variability), and an adaptation of the process noise variance (accounting for the *intra-specimen* variability). The following points summarize the algorithm operation, while Table 1 explains the variances involved in the algorithm.

1. Initialize the algorithm:

$$\begin{aligned} z_0 &\sim p(x_0^r, \sigma_{z_0}^2(x_0^r)) \\ \forall i = 1, \dots, N_S \\ \theta_0^{(i)} &\sim p(\theta_0, \sigma_{\theta_0}^2) \\ x_0^{(i)} &\sim p(x_0 | [z_0, \theta_0^{(i)}], \sigma_{x_0}^2) \\ w_0^{(i)} &= 1/N_S \end{aligned}$$

2. Perform the transition:

Update useful parameters

$$\begin{aligned} \sigma_{\xi_k}^2 &= \sigma_{\xi_0}^2 f(k) && \text{for artificial dynamics, or} \\ \zeta_k &= \zeta_0 f(k) && \text{for kernel smoothing} \\ \sigma_{\Lambda_k}^2 &= f(\sigma_{z_k}^2(x_k^r)) && \text{according to (19), or} \\ \sigma_{\Lambda_k}^2 &= f(\varphi_k, \sigma_{\Lambda_0}^2, \sigma_{\Lambda,max}^2, \sigma_{\Lambda,min}^2) && \text{according to (21)} \end{aligned}$$

$\forall i = 1, \dots, N_S$

$$\begin{aligned} \theta_k^{(i)} &\sim p(\theta_k | \theta_{k-1}^{(i)}, \sigma_{\xi_k}^2) && \text{for artificial dynamics, or} \\ \theta_k^{(i)} &\sim p(\theta_k | \mu_{\theta,k}^{(i)}, \zeta_k^2 \Sigma_{\theta,k-1}) && \text{for kernel smoothing} \\ x_k^{(i)} &\sim p(x_k | [x_{k-1}^{(i)}, \theta_k^{(i)}], \sigma_{x_{k-1}}^2) \end{aligned}$$

Draw

z_k using a simulated measurement system

3. Evaluate the new weights

$$w_k^{(i)} \propto w_{n,k-1}^{(i)} p(z_k | \mathbf{y}_k^{(i)} = [x_k^{(i)}, \theta_k^{(i)}])$$

$$w_{n,k}^{(i)} = \frac{w_k^{(i)}}{\sum_i w_k^{(i)}}$$

4. Evaluate the posterior pdf

$$p(\mathbf{y}_k | z_{1:k}) = \sum_i w_{n,k}^{(i)} \delta(\mathbf{y}_k - \mathbf{y}_k^{(i)})$$

If the kernel smoothing is adopted, the posterior pdf of parameters becomes:

$$p(\theta | z_{1:k}) = \sum_i w_{n,k}^{(i)} N(\theta | \mu_{\theta,k}^{(i)}, \zeta_k^2 \Sigma_{\theta,k})$$

5. Evaluate the Residual useful life up to the limit state x_{lim} .

$\forall i = 1, \dots, N_S$

- Estimate the theoretical number of remaining load cycles using Eq. (2b)

$$N_r^{(i)} = N_r(x_{lim}, x_0 = x_k^{(i)}, \theta_k^{(i)})$$

- Alter the estimation of the remaining load cycles using the integral of the random process Ω in (7):

$$N_r^{(i)} = \int_0^{N_r^{(i)}} \Omega dN = \sum_{j=1}^{n^* = \frac{N_r^{(i)}}{\Delta N}} \omega_j \Delta N$$

- Generate the posterior pdf of the remaining load cycles

$$p(N_r | z_{1:k}) = \sum_i w_{n,k}^{(i)} \delta(N_r - N_r^{(i)})$$

6. Resample the particles according to whatever resampling procedure: for instance the systematic resampling scheme (Arulampalam et al. 2002).

$\forall j = 1, \dots, N_S$ Assign: $y_k^{(j)} = y_k^{(i)}$ with probability $w_{n,k}^{(i)}$

7. Repeat the steps 2-6 for each k -th time step.

Table 1. Variances used to develop the SIR algorithm.

Variance	Description
$\sigma_{z,k^2}(x_k^r)$	Variance associated to the observations as a function of the real state x_k^r at the k -th step
σ_{ξ,k^2}	Variance associated to the parameter samples for the AD algorithm at the k -th step
σ_{x,k^2}	Variance associated to the state x coming from the state evolution equation at the k -th step
ζ_k	Smoothing parameter for KS algorithm at the general k -th step
σ_{A,σ^2}	Constant value associated to the noise variance
σ_{A,max^2}	Maximum allowable variance of the random noise A
σ_{A,min^2}	Minimum allowable variance of the random noise A
$\Sigma_{\theta,k}$	Monte Carlo variance of θ at the k -th step

4. PROGNOSIS OF THE FCG PHENOMENON

This section shows the SIR algorithm of section 3 applied to several simulated crack propagations. The key parameters of the algorithm are set according to the problem and the main features of the simulation are described as well.

4.1. Target crack growth

Target crack propagations are simulated according to Eq. (22) to prove the validity of the method. In this sub-section, the term a indicates the target crack, despite of the term x that indicates the crack samples drawn by the SIR algorithm. Table 2 shows the values of constants and parameters employed in the simulation.

$$a_k = a_{k-1} + \psi_0 C (F \Delta S \sqrt{\pi a_{k-1}})^m \omega_{k-1} \Delta N \quad (22)$$

The correction parameter ψ_0 modifies the theoretical crack propagation, and it constitutes the only parameter that has to be estimated through the SIR algorithm. It means that the vector θ describing the parameters of the model collapse to a single scalar quantity, ψ . Consequently, the vector of random processes ξ becomes scalar, too. Roughly speaking, a different correction parameter in the simulated crack increases or reduces the theoretical crack increment introduced by the Paris-Erdogan model. Several simulations are performed using different correction parameters. Figure 2 shows an example of crack propagation simulated according to the characteristics in Table 2 and in Eq. (22). The target crack length a altered by a normal random noise (driven by σ_{η}^2) constitutes the observation z provided to the SIR algorithm, visible in Eq. (23a).

The variance of the normal random noise is a function of the crack length itself multiplied by a constant α on the order of $1E-3$ as presented in Eq. (23b). This simulated measurement system is adopted in both the simulations with AD and KS approach.

Table 2. Features of the crack simulation.

Parameter	Description	Value
$F(x)$	Crack shape function [-]	1.2
ΔS	Applied fatigue load [MPa]	30
C	Empirical constant [mm/cycle · 1/MPa√mm]	2.382e-12
m	Empirical constant [-]	3.2
ψ_0	Correction parameter [-]	1.25
ω	Random noise	$\sim \log N(1, \exp\{2\} - 1)$
a_0	Starting crack length [mm]	5
a_{lim}	Critical crack length [mm]	100
ΔN	load cycle increment per time-step [cycles]	100

$$z_k = h(a_k, \eta_k) = a_k + N(0, \sigma_{\eta_k}^2) \quad (23a)$$

$$\sigma_{\eta_k}^2 = \alpha E(a_k)^2 \quad (23b)$$

In this case, the variance of the random process σ_{η,k^2} coincides to the variance of the measurement system given the Eq. (23a). As a consequence, $\sigma_{z,k^2} = \sigma_{\eta,k^2}$.

4.2. SIR algorithm with artificial dynamics

The monitoring-prediction problem of the FCG can be described combining the equations and ideas described in the previous sections. Equations (24a), (24b) and (24c) constitute the core of the SIR algorithm with the AD technique for the estimation of the model parameters.

$$x_k^{(i)} = x_{k-1}^{(i)} + \psi_{k-1}^{(i)} C \left(F \Delta S \sqrt{\pi x_{k-1}^{(i)}} \right)^m \omega_{k-1}^{(i)} \Delta N \quad (24a)$$

$$\log \psi_k^{(i)} = \log \psi_{k-1}^{(i)} + \xi_k^{(i)} \quad (24b)$$

$$z_k = a_k + \eta_k \quad (24c)$$

The superscript (i) indicates the i -th particle of the algorithm. Moreover, since the crack can only increase over time, the parameter ψ should be log-normally distributed so that the values cannot be negative. Therefore, the logarithmic transformation allows computing the *artificial dynamics* method by means of a normally distributed noise ξ . Equations (25) show the random processes used during the filtering procedure. The random process affecting the measures is the same just described in the Eqs. (23).

$$\omega_k = \exp\{\lambda_k\}; \lambda_k \sim N\left(\mu_{\lambda_k} = -\frac{\sigma_{\eta_k}^2}{2}, \sigma_{\lambda_k}^2 = \sigma_{\eta_k}^2\right) \quad (25a)$$

$$\xi_k \sim N\left(0, \sigma_{\xi_k}^2 = \sigma_{\xi_0}^2 f(k)\right) \quad (25b)$$

$$\eta_k \sim N\left(0, \sigma_{\eta_k}^2 = \alpha E(a_k)^2\right) \quad (25c)$$

Equation (25a) shows the variance of the ancillary quantity \mathcal{A} (used to define the random process ω_k) as presented in Eq. (19). The *artificial dynamics* for the parameter estimation is generated using a normal random noise as in Eq. (25b) with decreasing variance defined in section 4.4.

4.3. SIR algorithm with kernel smoothing

Similarly to the formulation of the sub-section 4.2, Eq. (26) shows the DSS model of the algorithm using the KS approach for the parameter estimation.

$$x_k^{(i)} = x_{k-1}^{(i)} + \psi_{k-1}^{(i)} C \left(F \Delta S \sqrt{\pi x_{k-1}^{(i)}} \right)^m \omega_{k-1}^{(i)} \Delta N \quad (26a)$$

$$\log \psi_k^{(i)} = \mu_{\log \psi, k}^{(i)} + \zeta_k \sqrt{\sigma_{\log \psi, k-1}^2} N(0,1) \quad (26b)$$

$$z_k = a_k + \eta_k \quad (26c)$$

$\sigma_{\log \psi, k-1}^2$ is the estimated variance of $\log \psi$ at the previous time-step. The term μ_{ψ}^k is the kernel location at step k and it is represented hereafter in scalar form (27).

$$\mu_{\log \psi, k}^{(i)} = b \log \psi_k^{(i)} + (1-b) E(\log \psi_k) \quad (27)$$

Where $b = \sqrt{1 - \zeta_k^2}$. All the other quantities follow the definitions of the previous sections. The random processes defining the noises are the following: the realizations of the state noise Ω follow Eq. (25a). The definition of $\sigma_{\mathcal{A}}^2$ is driven by the variance of the measurement system or by the *similarity parameter* of Xu and Li defined in (21), as in the case of artificial dynamics. The value of the smoothing parameter is presented in section 4.4.

4.4. On the influence of initial variances

As reminded in section 3, the *artificial dynamics* approach to estimate the model parameters needs a starting value for the variance used to draw the samples, which is $\sigma_{\xi, 0}^2$. Even the *kernel smoothing* approach requires the selection of the initial variance, but it is less important than the values employed in the AD algorithm. Actually, only the first samples of the parameters $\log \psi$ are drawn using the starting variance.

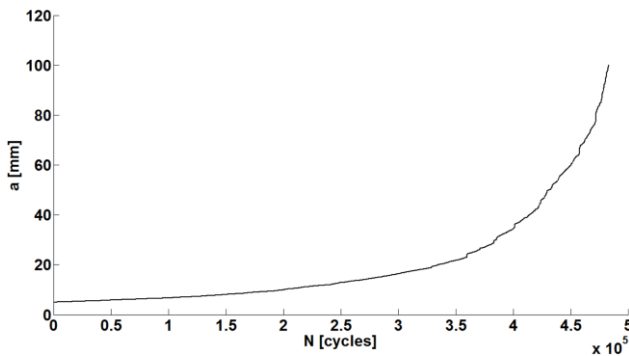


Figure 2. Example of target crack growth according to (22) and Table 2.

The Monte Carlo variance $\sigma_{\log \psi}^2$ of the previous time step and the smoothing parameter ζ govern the current sampling step. However, a wrong initial variance of the parameter pdf can affect the overall performance of the algorithm even using the KS approach. Besides, prognostic system requires the decreasing function $f(k)$ to update $\sigma_{\xi, k}^2$ and ζ_k , respectively. The values presented afterwards have been preliminary selected following a *trial & error* procedure. These values must not be regarded as the best in absolute terms; nevertheless, they are associated to fairly good performances of the algorithm. A sensitivity analysis of SIR performances with respect to initialization values is matter of future research by the authors.

The quantities presented here represent reasonable values according to the other parameter values, the variability associated to the observations and the magnitude of the observed state x . As declared above, they cannot be considered optimal, nor suboptimal variances for the studied process. Equation (28a) shows the starting values employed for the parameter noise variance with both the AD and KS technique, while Eq. (28b) shows the decreasing variance for the *artificial dynamics*. Regarding the KS approach, the initial value and the sub-sequent values of the *smoothing parameters* are defined in (28c-d).

$$\sigma_{\xi, 0}^2 = 0.1 \quad (28a)$$

$$\sigma_{\xi, k}^2 = \frac{\sigma_{\xi, 0}^2}{k} \quad (28b)$$

$$\zeta_0 = 1 \quad (28c)$$

$$\zeta_k = \frac{1}{\sqrt{k}} \quad (28d)$$

The starting variances of the random noise ω conditioning the state evolution is selected with the same *trial & error* approach. Nevertheless, if the method based on Eq. (19) is adopted, the tuning of the initial variance is not required. As a matter of fact, the variance $\sigma_{\mathcal{A}}^2$ is associated to the observation variance from the first measure. The approach proposed by Xu & Li requires the selection of three quantities instead: $\sigma_{\mathcal{A}, 0}^2$, $\sigma_{\mathcal{A}, min}^2$ and $\sigma_{\mathcal{A}, max}^2$. The magnitudes used in the simulations are expressed in Eq. (29) and can be considered reasonable values for the studied damage propagation process.

$$\sigma_{\Lambda, 0}^2 = 1 \quad (29a)$$

$$\sigma_{\Lambda, max}^2 = 1.5 \quad (29b)$$

$$\sigma_{\Lambda, min}^2 = 0.2 \quad (29c)$$

These values are used for both the AD and the KS algorithms. It has to be noticed that the term $\sigma_{\mathcal{A}, 0}^2$ is not the actual variance associated to the random noise, because it has multiplied by $\sqrt{1/\varphi}$, as presented in (21).

5. RESULTS

This section contains the main results of the algorithm. The capability of the developed prognostic unit to assess the residual lifetime of the system is highlighted in terms of model parameter estimation and RUL pdf. The overall behavior of the algorithm is established using both the AD and the KS technique. The crack length monitoring is simulated up to 150000 load cycles, which corresponds to a crack increment of around 7 mm: from 5 mm to 12 mm. The number of employed particles is 5000, the ΔN is set to 100 load cycles, and a measure of the crack length z becomes available every ΔN . During these 150000 load cycles, the algorithms try to estimate the most probable crack length (state of the system), the *correction parameter* ψ , and the remaining number of cycles before the critical crack length limit (here arbitrary set to 100 mm).

5.1. Monitoring and prediction of FCG

The estimation of the crack length is the easiest goal because of the construction of the algorithm itself. Almost every estimation of the state contains the actual state, and the results are comparable for both the KS and the AD. The results are satisfactory and do not constitute the nodal point of the proposed algorithm. Then, the following parts will focus on the estimation capabilities in terms of correction parameter and RUL probability density functions.

Figures 3 and 4 shows the results of the algorithm using the *artificial dynamics* approach to estimate the parameter ψ and the RUL, respectively. The simulations involve a small crack increment (from 5 to 12 millimeters) with respect to the critical crack length (100 mm), and the algorithm uses many measures to achieve acceptable results of the parameter ψ (expressed in Figure 3 in its logarithmic form), then adjusting the RUL prediction (Figure 4).

However, the crack increment Δx is very small in the first part of the crack propagation so that the discrimination among good and wrong values of the *correction parameter* is difficult.

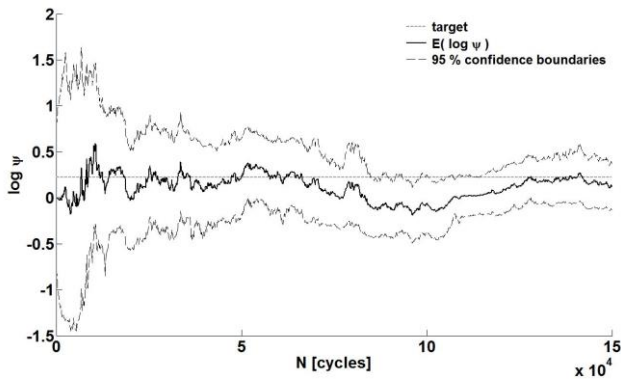


Figure 3. *Correction parameter* ($\log \psi$) estimation using the SIR algorithm with *artificial dynamics*.

Above all, the convergence velocity depends on the scatter affecting the measures. Hence, less frequent measures provided with larger ΔN could produce the same results because the difference between two distant crack lengths makes easier the identification of good and bad parameter values.

The results of the previous figures have been achieved using the variance updating in (19), in which the variance of the observation equation governs the variance of the process noise σ_A^2 . The implementation of the *similarity parameter* to drive the variance σ_A^2 produces comparable results.

Figure 5 and 6 show the same graphs using a SIR algorithm with the *kernel smoothing* method. As expected, the smoothness of these results is higher with respect to the *artificial dynamics* case where, actually, the smoothing is missing. The advantages of the *kernel smoothing* technique is clear looking at the results of the whole simulation. The KS algorithm produces more stable results in terms of parameter estimation and above all RUL prediction with respect to the *artificial dynamics* method.

The results of the *kernel smoothing* algorithm relate to the adaptive noise variance in (21), using the similarity parameter proposed by Xu and Li. It is important to underline that the first approach using the same variance of the observation equation does not work in this case. This can be related to the measure variance which is too small with respect to the one required by the algorithm. Figure 7 shows the estimation of the correction parameter using the *kernel smoothing* approach with the adaptive variance of the process noise according to (19).

It obviously produces a wrong RUL prediction. The problem does not appear in the *artificial dynamics* case, where the artificial noise added to the particles is independent from whatever previous estimation. This leads to an higher scatter of the particles with respect to the *kernel smoothing* case.

Therefore, a small variance of ω does not decrease the performance in a marked way.

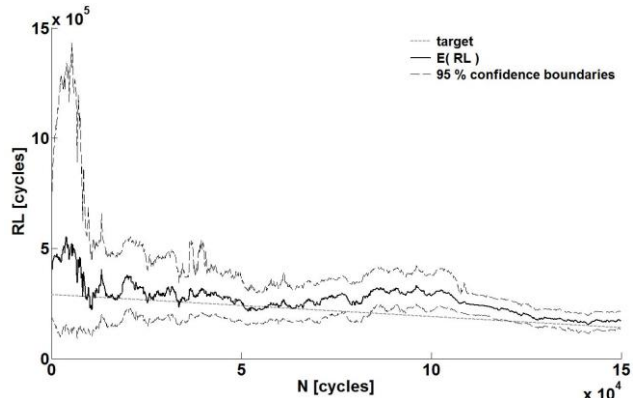


Figure 4. *Residual useful life* estimation using the SIR algorithm with *artificial dynamics*.

The approach of Xu and Li based on the *similarity* between the state estimation and the observations seems better as it works with both the algorithms. However, the tuning of $\sigma_{\Lambda, \max}^2$, $\sigma_{\Lambda, \min}^2$ and above all $\sigma_{\Lambda, 0}^2$ is solved here with a *trial & error* procedure. One more question has to be investigated: the capability of the algorithm with one adaptive parameter only (ψ), to predict the RUL of a simulated crack built with a different couple of parameters C and m instead of a different value of ψ only. Then, a fictitious crack growth is simulated using $(C; m) = (2.39e-11; 2.9)$ instead of the values presented in Table 2. In this case, the results are compared in terms of RUL distributions only because the *correction parameter* ψ , assumes a value which is not comparable with a target. Figure 9 and 10 show the RUL prediction of the latter case for the *artificial dynamics* and the *kernel smoothing* algorithm, respectively. Even in this case, the variance of the random process is set equal to the variance of the observations for the AD and the *similarity parameter* has been employed for the KS approach, respectively. However, the initial variance of the correction parameter, defined as $\sigma_{\psi, 0}^2$, has to be properly tuned and differs from the case where a different ψ_0 drives the target crack growth. As visible in the comparison between the figures 4-8 and 6-9, the results remain good. Of course, the validity of the results is limited to the range of crack lengths adopted in these simulations.

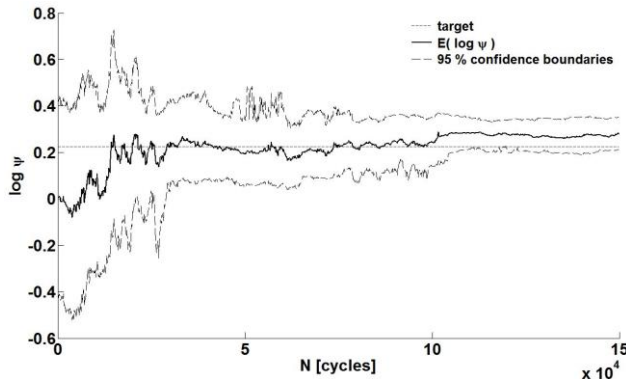


Figure 5. Estimation of the *correction parameter* ($\log \psi$) using the *kernel smoothing* algorithm.

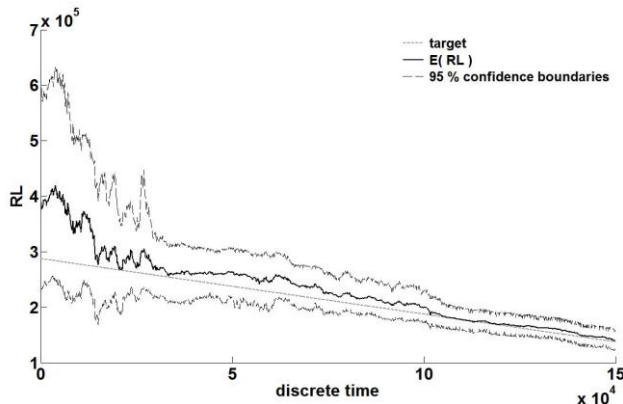


Figure 6. Estimation of the RUL using the *kernel smoothing* algorithm.

The performances outside this range must be investigated. The AD algorithm produces worse results with respect to the previous case, while the kernel smoothing converges to a slightly biased expected value. This small bias does not appear when the target crack is built with a different parameter ψ . Nonetheless, the estimations remain acceptable. All the analyses and results presented above can be considered a preliminary study of the matter. Of course, they do not have the intent to quantify the errors occurring during the filtering procedure performed by the SIR algorithm. They want to investigate the effectiveness of the proposed methods and to analyze the performances as a tradeoff between different approaches.

6. CONCLUSION

A prognostic unit for FCG grounding on sequential Monte Carlo algorithms has been developed in this work. The *kernel smoothing* technique introduces more stable parameter estimation and RUL prediction. Its disadvantage is the higher computational effort with respect to the *artificial dynamics* algorithm. The estimation of the remaining number of cycles N_r using the stochastic integral proposed by Yang & Manning (1996) drastically reduces the computational effort required by common SIR algorithms for FCG prediction. Reporting on the adaptive variance of the process noise, the simple method that links the variance of the random process with the variance of the measurement system does not work in general terms, since the results are good only in the case of *artificial dynamics* algorithm. The approach based on the *similarity parameter* produces better results provided that the constant parameter $\sigma_{\Lambda, 0}^2$ and the maximum and minimum allowable variances are properly selected. Actually, the tuning of all the parameters introduced in the mathematical formulation is a non-negligible limitation of the algorithm. Although the work highlighted some issues not already solved, the preliminary analysis presented here shows promising results. The authors want to stress the attention on the different kind of uncertainties that can affect the damage propagation process and on the proposed solution, introducing the *inter-specimen* and the *intra-specimen* variability within a Bayesian filtering framework. On the other hand, several investigations are mandatory to understand the behavior of the proposed sequential Monte Carlo algorithm. The validity of the *correction parameters* to cover the *inter-specimen* variability driven by multiple parameters (for example C and m) has to be proved, even though the results presented in section 5 seems good. Then, an in-depth study of the variances involved in the process could bring to *self-adaptive algorithms* in which the influence of the selection of the initial variances is very limited. Finally yet importantly, the testing of the proposed system on real structures is fundamental to prove the effectiveness of the method. The implementation of the methodology on real structures remains prohibitive especially because of the difficulties to deal with random load conditions. Even though the scientific

community has developed many approaches to solve the problem using efficient statistical ways, the implementation of these methods into a real-time prognostics framework introduces additional complications. For instance the real-time estimation of the loads close to the damage, or the implementation of time-varying variables in the RUL prediction. These questions add up to the current issues of model parameter estimation and optimal variance selection, enlarging the dimension of the prognostic problem.

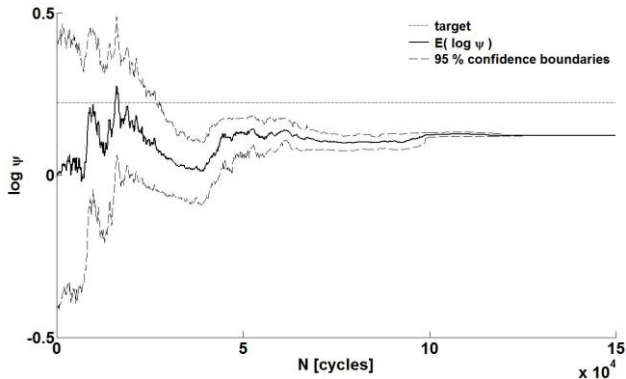


Figure 7. Wrong estimation of the *correction parameter* ($\log \psi$) using the KS algorithm and a noise variance equal to the variance of the measurement system.

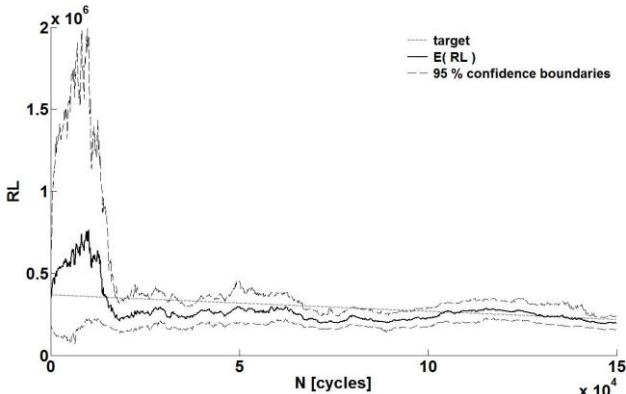


Figure 8. RUL prediction with *artificial dynamics* algorithm, using a target crack built with different C and m parameters.

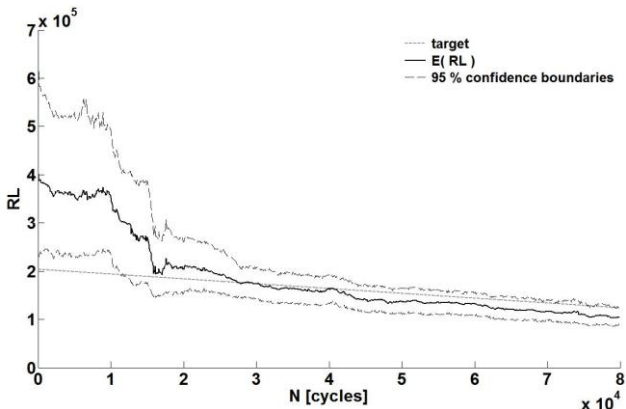


Figure 9. RUL prediction with *kernel smoothing* algorithm, using a target crack built with different C and m parameters.

REFERENCES

Arulampalam, M. S., Maskell, S., Gordon, N., Clapp, T. (2002). A Tutorial on Particle Filters for Online Nonlinear/Non-Gaussian Bayesian Tracking. *IEEE Trans on Signal Processing*, 50(2), pp. 174-188.

Bourinet J.M., Lemaire, M. (2008). Form sensitivities to correlation: application to fatigue crack propagation based on Virkler’s data. *4th International ASRANet colloquium*, Athens.

Broek, D. (1988). *The practical use of fracture mechanics*. Netherlands: Kluwer Academic Publishers.

Cadini, F., Zio, E., Avram, D. (2009). Monte Carlo-based filtering for fatigue crack growth estimation. *Probabilist Eng Mech*, 24, pp. 367-373.

Chiachio, J., Chiachio, M., Saxena, A., Rus, G., Goebel, K. (2013). An Energy-Based Prognostics Framework to Predict Fatigue Damage Evolution in Composites. *Annual Conference of the Prognostics and Health Management Society*, October, 14-17, New Orleans, LA.

Corbetta, M., Sbarufatti, C., Manes, A., Giglio, M. (2013a). Stochastic definition of state-space equation for particle filtering algorithms. *Chem Eng Trans*, 33, pp. 1075-1080.

Corbetta, M., Sbarufatti, C., Manes, A., Giglio, M. (2013b). On-line updating of dynamic state-space model for Bayesian filtering through Markov chain Monte Carlo techniques. *Chem Eng Trans*, 33, pp. 133-138.

Corbetta, M., Sbarufatti, C., Manes, A., Giglio, M. (2014). On dynamic state-space models for fatigue induced structural degradation. *Int J Fatigue*, 61, pp. 202-219.

Cross, R., Makeev, A., Armanios, E. (2007). Simultaneous uncertainty quantification of fracture mechanics based life prediction model parameters. *Int J Fatigue*, 29, pp. 1510-1515.

Daigle, M., Goebel, K. (2011). Multiple damage progression paths in model-based prognostics. In *Aerospace conference, 2011 IEEE*, pp. 1-10.

Doucet, A., Godsill, S., Andrieu, C. (2000). On sequential Monte Carlo sampling methods for Bayesian filtering. *Statistics and Computing*, 10, pp. 197-208.

Elber, W. (1970). Fatigue crack closure under cyclic tension. *Eng Frac Mech*, 2, pp.37-45.

Elber, W. (1971). The significance of crack closure. In ASTM STP 486, American Society for Testing and Materials, *Damage Tolerance in Aircraft Structures* (pp. 230-242). Philadelphia PA.

Haug, A.J. (2005). A tutorial on Bayesian estimation and tracking techniques applicable to nonlinear and non-Gaussian processes. *MITRE technical report*, MITRE McLean, Virginia.

Kantas, N., Doucet, A., Singh, S.S., Maciejowski, J.M. (2009). An overview of Sequential Monte Carlo Methods for Parameter Estimation in General State-Space Models. In *15th ifac symposium on system identification* (Vol. 15).

- Liu, J.S., West, M. (2001). Combined parameter and state estimation in simulation-based filtering. In Doucet, A., De Freitas, J.F.G., Gordon, N.J., (Eds.), *Sequential Monte Carlo Methods in Practice*. New York: Springer-Verlag.
- Gordon, N. J., Salmond, D. J., Smith, A. F. M. (1993). Novel approach to non-linear/non-Gaussian Bayesian state estimation, *IEEE Proceedings F (Radar and Signal Processing)*, 140(2), pp. 107-113.
- Mattrand, C., Bourinet, J. M. (2011). Random load sequences and stochastic crack growth based on measured load data. *Eng Fract Mech*, 78, pp. 3030-3048.
- NASA J.S. Centre and Southwest Research Institute. (2002). *NASGRO reference manual*, Version 4.02.
- Newman Jr., J. C. (1981). A crack-closure model for predicting fatigue crack growth under aircraft spectrum loading. *ASTM STP*, 748, pp.53-84.
- Newman Jr., J. C., (2005). Crack growth predictions in aluminum and titanium alloys under aircraft load spectra. In: *Proceedings of the XIth international conference of fracture*, Turin, Italy.
- Newman Jr., J. C., Irving, P.E., Lin, J., Le, D., D. (2006). Crack growth predictions in a complex helicopter component under spectrum loading. *Fatigue Fract Eng Mater Struct*, 29, pp. 949-958.
- Paris, P.C., Erdogan, F. (1963). A critical analysis of crack propagation laws. *Trans ASME – J Basic Eng*, 85, pp. 528-534.
- Ray, A., Patankar, R. (1999). A stochastic model of fatigue crack propagation under variable-amplitude loading. *Eng Fract Mech*, 62, pp. 477-493.
- Scafetta, N., Ray, A., West, B. J. (2006). Correlation regimes in fluctuations of fatigue crack growth. *Physica A*, 359, pp. 1-23.
- Virkler, D.A., Hillberry, B.M., Goel, P.K. (1978). The statistical nature of fatigue crack propagation. *Technical report*, Air Force Flight Dynamics Laboratory, AFFDL-TR-78-43.
- West, M. (1993). Mixture Models, Monte Carlo, Bayesian updating and dynamic models, In J. H. Newton (Ed.), *Computing Science and Statistics: Proceedings of the 24th symposium of the Interface*, pp. 325-333. Interface Foundation of North America, Fairfax Station, Virginia.
- Willenborg, J., Engle, R. M., Wood, H.A. (1971). A Crack Growth Retardation Model Using an Effective Stress Concept. *Technical Memorandum*, Air Force Flight Dynamics Laboratory, AFFDL-TM-71-1-FBR.
- Xu, X., Li, B. (2005). Rao-Blackwellised Particle Filter with Adaptive System Noise and its Evaluation for Tracking in Surveillance. In *2nd Joint IEEE International workshop on Visual Surveillance and Performance Evaluation of Tracking and Surveillance*, Oct 15-16, Beijing, China.
- Yang, J. N., Manning, S. D. (1996). A simple second order approximation for stochastic crack growth analysis. *Eng Fract Mech*, 53(5), pp. 677-686.

BIOGRAPHIES

Matteo Corbetta is a Ph.D. student in Mechanical Engineering at the Politecnico di Milano, Italy. He obtained the Bachelor and Master degrees in mechanical engineering both at the Politecnico di Milano in 2009 and 2012, respectively. He was a postgraduate research student in the mechanical department of the Politecnico di Milano in 2012. His Ph.D. thesis focuses on probabilistic modeling of airframe crack propagation for real-time failure prognosis and lifetime prediction using sensor networks. He is currently involved in lecturing as an assistant professor of machine design courses. He received a nomination for the best paper award at the 22th European Safety and Reliability conference (ESREL 2013).

Claudio Sbarufatti is a Post-Doctorate Research Scientist at the Department of Mechanics in the Politecnico di Milano, Italy. He obtained the master degree in Mechanical Engineering in 2009 and completed his Ph.D. studies in 2013 in Aerospace Engineering (Rotary Wing Aircraft), both at the Politecnico di Milano. The title of his Ph.D. thesis is “Fatigue crack monitoring of helicopter fuselages and life evaluation through sensor networks”, for which he received the European Label Ph.D. certificate cum laude. He is involved in the management of international projects mainly focused on Structural Health Monitoring. His main research topics are sensor network designs for damage and impact diagnosis, model-based SHM, prognosis of residual life under constant and variable loads, impact modeling on composite structures.

Andrea Manes is a Research Scientist and Assistant Professor at the Department of Mechanics in the Politecnico di Milano, Italy. He obtained a master degree in Aerospace Engineering and PhD in Mechanical Systems Engineering both at the Politecnico di Milano. His primary research topics are related to strength assessment of mechanical and aeronautical components under service and extreme load, Structural Health Monitoring and calibration of mechanical properties of metals and composite. His actual research fields are mainly focused within collaborative research projects in the framework of the European Defence Agency. He is the author of more than 100 papers presented in international journals and conferences.

Marco Giglio is the Associate Professor of Mechanical Design and Strength of Materials, and works in the Department of Mechanical Engineering at the Politecnico di Milano, Italy. His research fields are novel methods for SHM application, methods of fatigue strength assessment in mechanical components subjects to multiaxial state of stress, design and analysis of helicopter components with defects, ballistic damage and evaluation of the residual strength, optimization of structures for energy application. He is the author of more than 150 scientific papers in international journals and conferences and is a member of various scientific associations (AIAS, Italian Association for the Stress Analysis, IGF, Italian Group Fracture).